nature cell biology

Adaptive suppression of the ATF4–CHOP branch of the unfolded protein response by toll-like receptor signalling

Connie W. Woo[1,5], Dongying Cui[1,5], Jerry Arellano[1], Bernhard Dorweiler[1,4], Heather Harding[2], Katherine A. Fitzgerald[3], David Ron[2] and Ira Tabas[1,6]

The endoplasmic reticulum (ER) unfolded protein response (UPR) restores equilibrium to the ER, but prolonged expression of the UPR effector CHOP (GADD153) is cytotoxic. We found that CHOP expression induced by ER stress was suppressed by prior engagement of toll-like receptor (TLR) 3 or 4 through a TRIF-dependent pathway. TLR engagement did not suppress phosphorylation of PERK or eIF-2α, which are upstream of CHOP, but phospho-eIF-2α failed to promote translation of the CHOP activator ATF4. In mice subjected to systemic ER stress, pretreatment with low dose lipopolysaccharide (LPS), a TLR4 ligand, suppressed CHOP expression and apoptosis in splenic macrophages, renal tubule cells and hepatocytes, and prevented renal dysfunction and hepatosteatosis. This protective effect of LPS did not occur in *Trif*$^{-/-}$ mice or in wild-type mice in which CHOP expression was genetically restored. Thus, TRIF-mediated signals from TLRs selectively attenuate translational activation of ATF4 and its downstream target gene CHOP. We speculate that this mechanism evolved to promote survival of TLR-expressing cells that experience prolonged levels of physiological ER stress in the course of the host response to invading pathogens.

The UPR is an integrated signal transduction pathway that restores equilibrium to the ER undergoing physiological or pathophysiological unfolded protein stress[1]. The UPR is initiated by activation of three molecules, PERK, IRE1α and ATF6. Activation of PERK leads to the phosphorylation of eIF-2α, which suppresses translation initiation of most cellular proteins but promotes translation initiation of ATF4, leading to transcription of the ATF4 downstream target CHOP (GADD153). In most circumstances, the three known transducers of UPR are regulated by similar cues and are thus coordinately activated[1]. An exception to this rule is pathologically prolonged ER stress, which occurs in a variety of disease processes where sustained PERK–CHOP signalling leads to apoptosis[2–8]. However, there are situations in normal physiology in which ER stress is prolonged, and we wondered how the cell prevents prolonged expression of pro-apoptotic CHOP under these conditions. For example, the IRE1α–XBP-1 pathway is activated during B cell differentiation in plasma cells[9], but CHOP expression is low, and evidence suggests this low level of CHOP expression promotes B cell survival[10].

Another situation in which prolonged ER stress occurs is during the response of the host to invasive organisms, as exemplified by exposure of cells to LPS, which activates TLR4 (**A002296**) signalling through the MyD88–Mal and TRIF–TRAM adaptors. This activation results in the production of inflammatory cytokines and antimicrobial proteins[11]. Prolonged ER stress occurs during LPS–TLR4 signalling[12,13], which probably arises from a marked increase in protein synthesis. Thus, we wondered whether CHOP expression in this setting is also suppressed.

To test the hypothesis that TLR4 signalling might suppress CHOP expression during a sustained UPR response, macrophages were pretreated in the absence or presence of a low dose of LPS that does not induce ER stress and then subjected to conditions of ER stress, including accumulation of lipoprotein-derived cholesterol[4,14], tunicamycin, a glycosylation inhibitor[15], azetidine, a proline analogue[16] and arsenite, an inducer of cellular oxidant stress[17]. LPS pretreatment markedly decreased levels of CHOP protein (Fig. 1a), *CHOP* mRNA (Supplementary Information, Fig. S1a) and ATF4 protein (Fig. 1b). In a time course experiment (see explanation in legend to Supplementary Information, Fig. S1b), we found that the ability of LPS to suppress CHOP in ER-stressed macrophages is persistent and occurs regardless of whether LPS is added before or at the same time as the ER stressor.

Despite marked suppression of CHOP, LPS pretreatment of macrophages or MEFs did not significantly suppress tunicamycin-induced phospho-PERK or phospho-eIF-2α (Fig. 1c, d; Supplementary Information, S2b), which are upstream of CHOP. The eIF-2α phosphatase GADD34, which is regulated by CHOP and also by other processes[18,19], was not markedly suppressed by LPS pretreatment (Supplementary Information, Fig. S1d), indicating that lack of phospho-eIF-2α suppression is not simply caused by a decrease in GADD34. LPS pretreatment

[1]Departments of Medicine, Pathology & Cell Biology, and Physiology & Cellular Biophysics, Columbia University, New York, NY 10032, USA. [2]Kimmel Center for Biology and Medicine of the Skirball Institute, New York University School of Medicine, New York, NY 10016, USA. [3]Department of Medicine, The University of Massachusetts Medical School, Worcester, MA 01605, USA. [4]Department of Cardiothoracic & Vascular Surgery, University of Mainz, Mainz, Germany.
[5]These authors contributed equally to this study.
[6]Correspondence should be addressed to I.T. (e-mail: iat1@columbia.edu)

Received 23 April 2009; accepted 28 July 2009; published online 25 October 2009; DOI: 10.1038/ncb1996

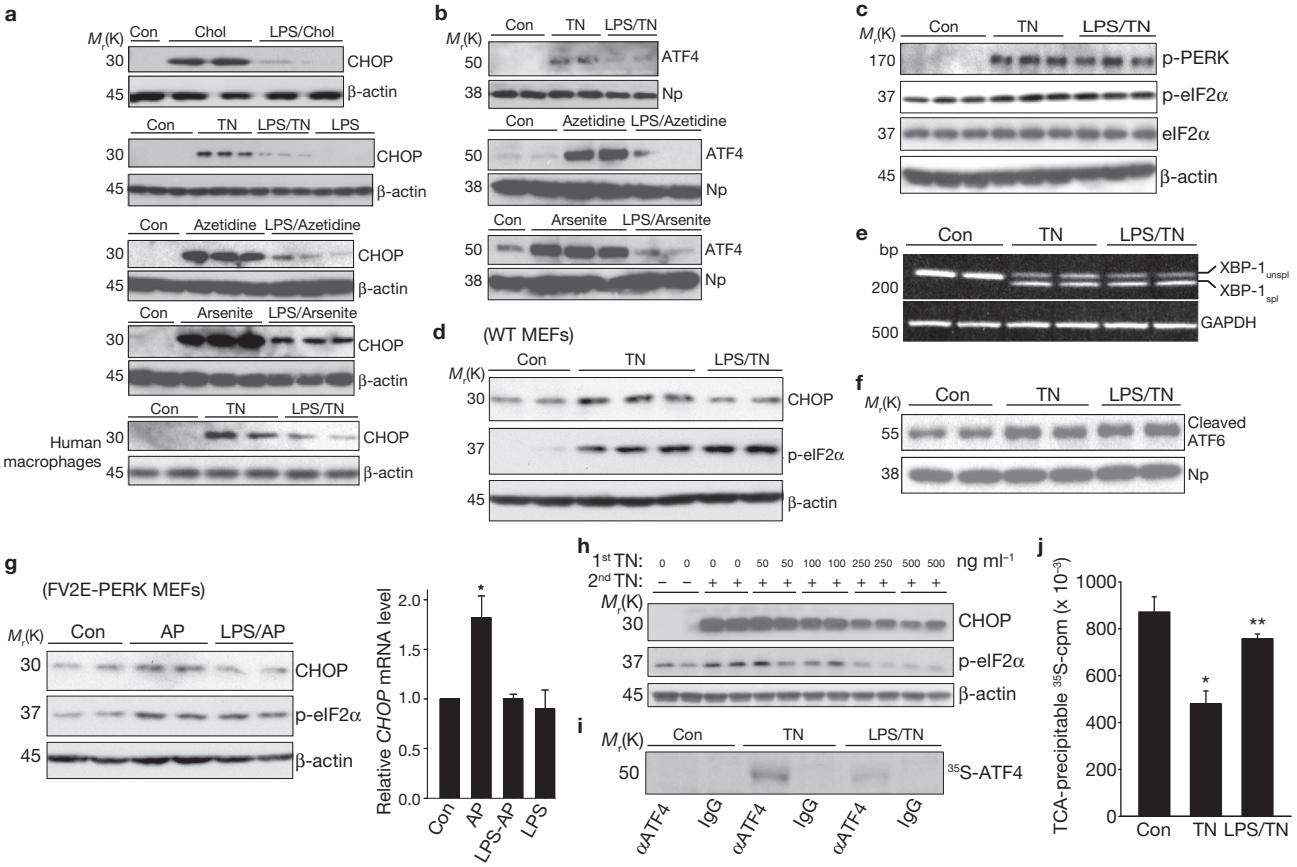

Figure 1 Pretreatment of macrophages with low dose LPS selectively suppresses the ATF4 –CHOP branch of the UPR. (**a**–**c**) Murine or human macrophages were untreated or pretreated with LPS (1 ng ml^{-1}) followed by cholesterol-loading (Chol) or 7-h treatment with tunicamycin (TN, 1 μg ml^{-1}), azetidine (1 mM) or arsenite (1 μM). Extracts of cells (**a**, **c**) or nuclei (**b**) were immunoblotted for the indicated UPR effectors or loading controls (Np, nucleophosmin). See Supplementary Information, Fig. S3 for full scans of selected blots in this and other figures. The phospho-eIF-2α:total eIF-2α densitometry ratios for Con, TN and LPS-TN were 0.66, 0.87, and 0.89, respectively (P <0.05 for TN, compared with Con, and LPS–TN, compared with Con). (**d**) Murine embryonic fibroblasts (MEFs) were incubated for 16 h in medium alone or in medium containing LPS (500 ng ml^{-1}). The cells were then treated for 2 h with tunicamycin, and then immunoblotted for CHOP, phospho-eIF-2α, or β-actin. (**e**) RNA from macrophages treated similarly to those in **c** was analysed by RT–PCR for unspliced (unspl) XBP-1, spliced (spl) XBP-1 and GAPDH. (**f**) Nuclear extracts from macrophages treated similarly to those in **c** were immunoblotted for ATF6 and nucleophosmin. The ATF6:Np densitometry ratios for Con, TN and LPS-TN were 0.76, 1.11 and 1.15, respectively. (**g**) FV2E-PERK MEFs were incubated for 16 h in medium with or without LPS (500 ng ml^{-1}) and then treated for 2 h with or without AP20187 (AP, 2 nM) to activate FV2E-PERK. Lysates were immunoblotted for CHOP, phospho-eIF-2α and β-actin. The CHOP:β-actin densitometry ratios for Con, AP and LPS-AP were 0.44, 0.74 and 0.44, respectively; the phospho-eIF-2α:β-actin ratios were 0.44, 0.88 and 0.97. RNA was assayed for *CHOP* mRNA by QT–PCR (*P <0.01, compared with other values). (**h**) Macrophages were pre-incubated for 24 h with the indicated concentrations of tunicamycin and then treated for 16 h with tunicamycin (1 μg ml^{-1}). Cell extracts were immunoblotted for CHOP, phospho-eIF2α, and β-actin. (**i**) Macrophages treated similarly to those in **c** were pulse-labelled with ^{35}S-methionine-cysteine for 20 min, followed by control (IgG) or anti-ATF4 immunoprecipitation. Autoradiograms of SDS–PAGE gels are shown. (**j**) Proteins from cells labelled as above were precipitated with ice-cold TCA and counted for ^{35}S cpm. For bar graphs in panels **g** and **j**, data are presented as mean ± s.e.m., n = 3. *P <0.01, compared with Con; **P <0.001, compared with TN.

also did not suppress the other two branches of the UPR, as indicated by similar XBP-1 splicing and cleaved nuclear ATF6 in LPS-pretreated cells, compared with ER-stressed cells (Fig. 1e, f). Phosphorylation of IRE1α, which is upstream of XBP-1 splicing, and expression of three chaperones downstream of XBP-1—grp78, calnexin, and calreticulin—were also not suppressed by LPS pretreatment (data not shown). Thus, LPS suppresses ATF4 and CHOP in a highly selective manner.

To determine whether suppression of CHOP was coupled to ER stress *per se,* we used a genetically altered MEF-based model described previously[20]. In this model, PERK is replaced by a cytoplasmic protein (FV2E-PERK), which dimerizes on exposure to cell-permeant AP20187 (AP), leading to eIF-2α phosphorylation in the absence of ER stress. We found that AP-induced CHOP was suppressed by pretreatment with LPS (Fig. 1g). Thus, the ability of LPS pretreatment to suppress CHOP is uncoupled to ER stress *per se*, consistent with the finding that the process is not mediated by suppression of the PERK–phospho-eIF-2α pathway. Moreover, the pathway cannot be explained by 'preconditioning', whereupon cells pre-exposed to modest ER stress become relatively resistant to subsequent UPR activation[6], as ER stress is not induced by 1 ng ml^{-1} LPS in macrophages (Fig. 1a; Supplementary Information, Fig. S2), and preconditioning, in contrast to the pathway described here, is associated with suppression of all three branches of the UPR[6], including phospho-eIF-2α (Fig. 1h).

As expected[21,22], *ATF4* mRNA did not change with tunicamycin treatment and we found that *ATF4* mRNA levels were not significantly altered by pretreatment with LPS (Supplementary Information, Fig. S1c). Despite stable levels of *ATF4* mRNA, the incorporation of ^{35}S-methionine-cysteine

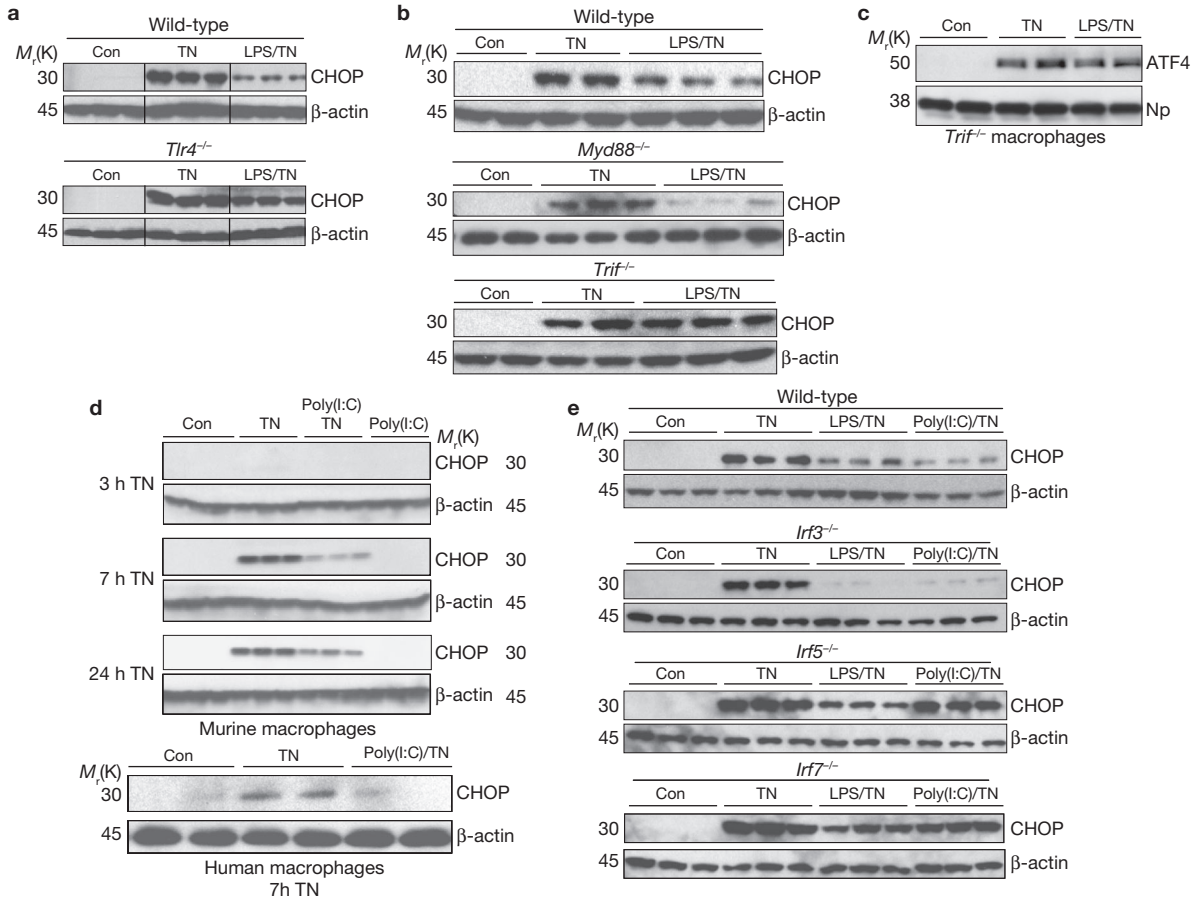

Figure 2 The ability of low dose LPS to suppress tunicamycin-induced CHOP is dependent on the TRIF branch of TLR signalling. (**a**, **b**, **e**), Bone marrow-derived macrophages from wild-type or the indicated gene-targeted mice were pre-incubated for 24 h in control medium or medium containing LPS (1 ng ml^{-1}) and then incubated for 10 h with medium alone or medium containing tunicamycin (1 ng ml^{-1}). The cells were then immunoblotted for CHOP and β-actin. (**c**) Macrophages from *Trif*$^{-/-}$ mice were pre-incubated for 24 h in the absence or presence of LPS (1 ng ml^{-1}) and then treated in the absence or presence of tunicamycin (TN, 1 μg ml^{-1}). Nuclear extracts were immunoblotted for ATF4 and nucleophosmin (Np) as a loading control. This experiment was conducted in parallel with, and should be compared with, the experiment with wild-type macrophages in Fig. 1b, top blot. (**d**) Murine peritoneal macrophages or human THP-1 cell-derived macrophages were pretreated for 24 h with 2.5 μg ml^{-1} poly(I:C) instead of LPS and then incubated with tunicamycin for the indicated times and immunoblotted for CHOP and β-actin as above. (**e**) As in panels **a** and **b** for the indicated gene-targeted mice, using either LPS or poly(I:C) pre-incubation.

into ATF4 protein after a 20-min labelling period was markedly reduced when exposure to tunicamycin was preceded by LPS (Fig. 1i). Given the brevity of the labelling period, this observation suggests that LPS affects rates of *ATF4* translation and not protein stability. An effect of LPS on ER stress-mediated translational control is further supported by the observation that LPS pretreatment interfered with suppression of global protein synthesis, which is normally observed after induction of ER stress (Fig. 1j). The global protein data also indicate that the decrease in ^{35}S-labelled ATF4 in the LPS-tunicamycin-treated cells cannot be explained by dilution of the radiolabelled charged tRNA(Met) pool. These data suggest that LPS pretreated cells become 'resistant' to the translational effects of phospho-eIF-2α, which both prevents ATF4–CHOP expression and maintains global protein synthesis.

We used peritoneal macrophages from a series of gene-targeted mice to map the TLR pathway involved in suppression of CHOP by LPS pretreatment. The marked suppression of CHOP by LPS in wild-type macrophages was almost completely absent in *Tlr4*$^{-/-}$ and *Trif*$^{-/-}$ macrophages, but not in *Myd88*$^{-/-}$ macrophages (Fig. 2a–c). Similar data were observed with macrophages from *Tram*$^{-/-}$ mice (data not shown). Furthermore, pretreatment of macrophages with the TLR3 (**A002295**) ligand poly(I:C), which only uses TRIF signalling[11], markedly suppressed tunicamycin-induced CHOP expression (Fig. 2d).

A major signal transducer downstream of the TRIF branch is IRF3, which subsequently induces expression of type 1 interferons[11]. However, macrophages from *Irf3*$^{-/-}$ mice showed normal suppression of tunicamycin-induced CHOP by LPS or poly(I:C) pretreatment (Fig. 2e, upper blots). Moreover, immunoneutralization of interferon-α and interferon-β had no effect on CHOP suppression (data not shown). Consistent with this finding, siRNA-mediated silencing of TANK-binding kinase 1 (TBK1), a kinase that mediates TRIF signalling[11], did not block suppression of CHOP by LPS (data not shown). Two other signal transducers that can be downstream of TRIF during TLR3 or TLR4 signalling are IRF5 and IRF7[23–25]. LPS, and especially poly(I:C), were unable to fully suppress tunicamycin-induced CHOP in macrophages deficient in either of these molecules (Fig. 2e, lower blots). In summary, LPS and poly(I:C) suppress CHOP in ER-stressed macrophages through a TLR–TRIF pathway that probably involves IRF5 and IRF7 but not IRF3.

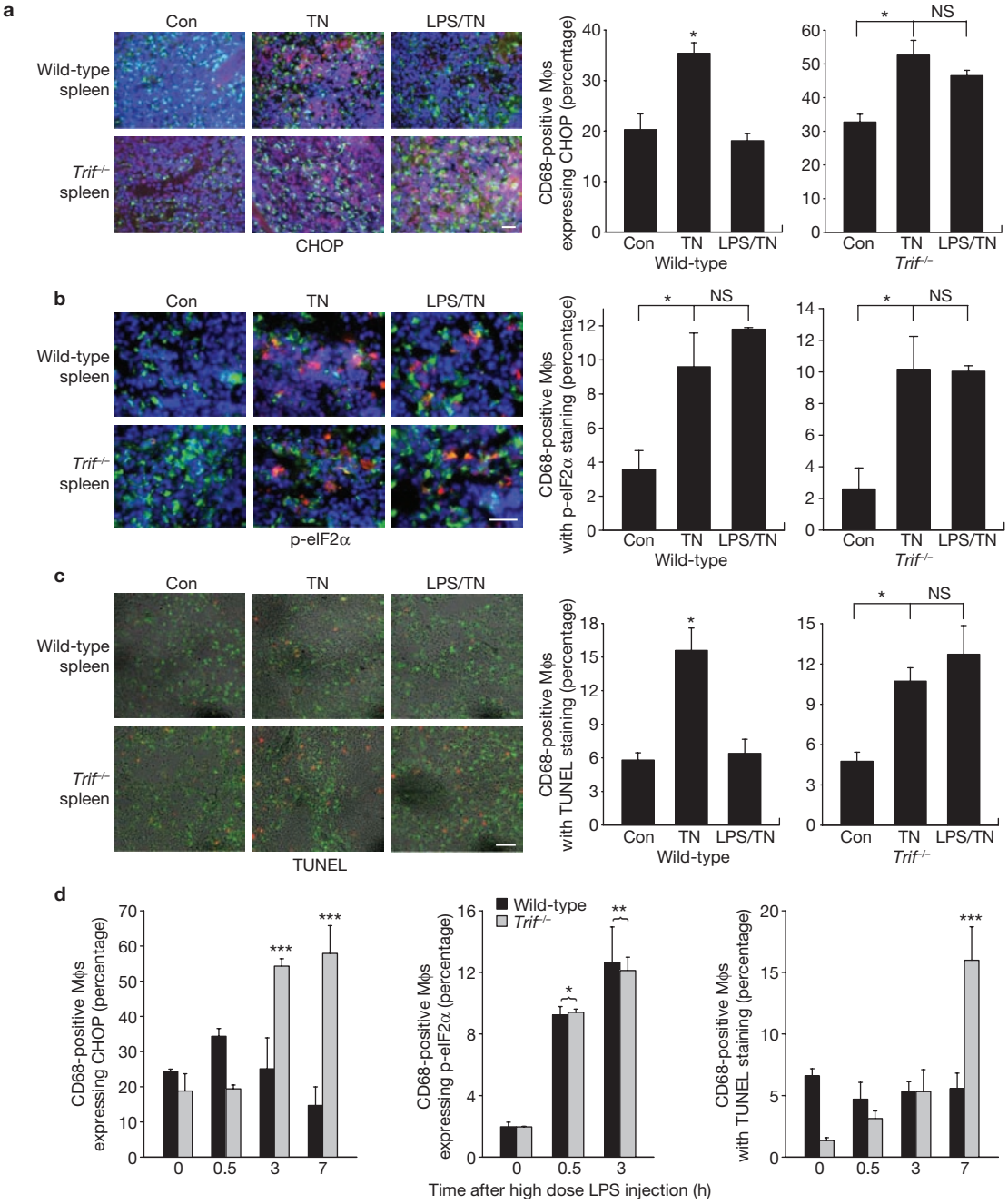

Figure 3 LPS treatment of tunicamycin-treated mice suppresses CHOP expression in splenic macrophages. (**a**, **b**) Wild-type or *Trif*$^{-/-}$ mice were injected intravenously with LPS (80 μg kg^{-1}) or vehicle control for 2 consecutive days. Mice were then injected with tunicamycin (TN, 1 mg kg^{-1}) intraperitoneally and killed 12 h later. Spleen cryosections were stained for (**a**) CHOP (red), CD68 as a macrophage marker (green) and DAPI as a stain for nuclei (blue); (**b**) phospho-eIF-2α (red in cytoplasm), CD68 (green), and DAPI (blue); or (**c**) TUNEL (red) and CD68 (green). Scale bars, 20 μm. Quantification of percent of CD68-positive macrophages that stained positively for CHOP, phospho-eIF-2α or TUNEL are shown in the bar graphs in **a** and **b**, respectively (*P <0.05; NS, nonsignificant). (**d**) CHOP expression and apoptosis in splenic macrophages are suppressed in a TRIF-dependent manner in mice treated with high dose LPS. Wild-type or *Trif*$^{-/-}$ mice were injected intraperitoneally with LPS (5 mg kg^{-1}) or vehicle control. At the indicated time-points, CD68-positive splenic cells were assayed for phospho-eIF-2α, CHOP expression and TUNEL-positive cells. *P <0.02, compared with zero time-point for both wild-type and *Trif*$^{-/-}$; **P <0.05, compared with zero time-point for both wild-type and *Trif*$^{-/-}$; ***P <0.05 for *Trif*$^{-/-}$, compared with both wild-type and *Trif*$^{-/-}$ at zero time-point and for wild-type at the same time-point. For all bar graphs, data are presented as mean ± s.e.m., n = 4.

To test this pathway *in vivo*, wild-type and *Trif*$^{-/-}$ mice were pretreated with of LPS (80 μg kg^{-1} day^{-1}), which did not cause any observable adverse effects in the mice, or vehicle control for two consecutive days and then exposed to an intraperitoneal injection of tunicamycin for 12 h to induce systemic ER stress[2]. CHOP was induced in macrophages by tunicamycin treatment, and LPS suppressed this induction in wild-type but not *Trif*$^{-/-}$ mice (Fig. 3a). Importantly, LPS pretreatment did not suppress phospho-eIF-2α (Fig. 3b), consistent with the mechanism elucidated in cultured cells (above). Apoptosis, as assessed by TUNEL staining, followed the same pattern as CHOP,

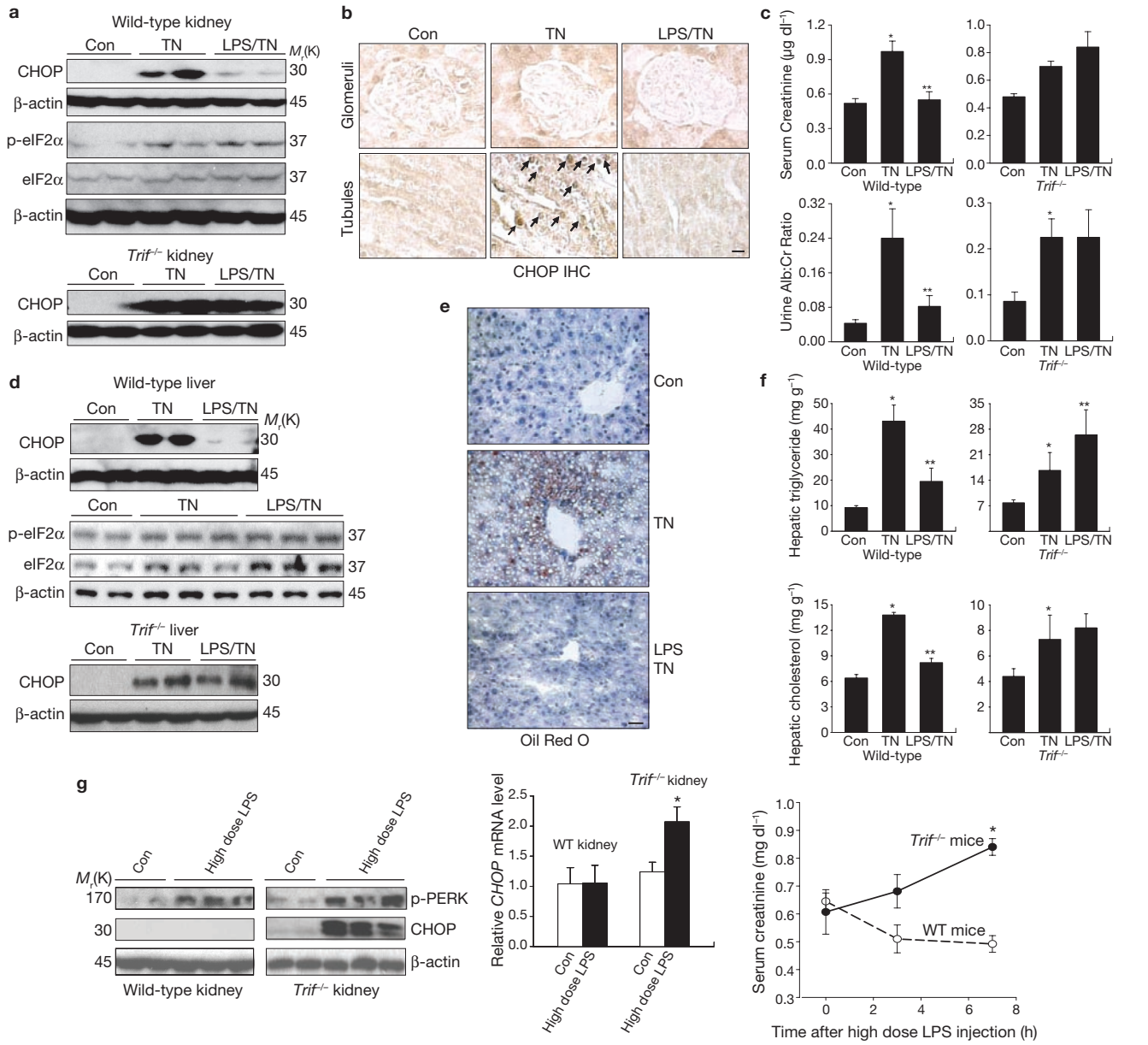

Figure 4 LPS treatment of tunicamycin-treated mice suppresses renal tubular and hepatic CHOP induction, renal dysfunction, and hepatosteatosis. Wild-type or *Trif*$^{-/-}$ mice were injected intravenously with LPS (80 μg kg^{-1}) or vehicle control intravenously for 2 consecutive days (note, in this experiment, the *Trif*$^{-/-}$ mice also had a deficiency of its co-adaptor TRAM; cells from *Trif*$^{-/-}$, *Tram*$^{-/-}$ and *Trif*$^{-/-}$*Tram*$^{-/-}$ mice behave similarly in terms of CHOP suppression by LPS pretreatment). Mice were then injected with tunicamycin (TN, 1 mg kg^{-1}) intraperitoneally and killed 48 h later. (**a**, **b**) Kidney extracts were assayed for CHOP, phospho-eIF-2α, and total eIF-2α expression, and kidney sections were immunostained for CHOP (CHOP IHC). The average phospho-eIF-2α:total eIF-2α densitometry ratios for the Con, TN, and LPS-TN groups were 0.26, 0.59, and 0.56, respectively (**a**). Arrows depict CHOP-positive nuclei in renal tubular cells (**b**). Scale bar, 10 μm. (**c**) Serum creatinine levels and urine albumin levels (normalized to urine creatinine) were determined for all groups of mice. **P* <0.01, compared with Con; ***P* <0.001, compared with TN. (**d**–**f**) The livers were assayed for CHOP, phospho-eIF-2α, and total eIF-2α expression; Oil Red O staining; and triglyceride and cholesterol mass. The average phospho-eIF-2α:total eIF-2α densitometry ratios for the Con, TN, and LPS-TN groups were 0.59, 0.64, and 0.86, respectively (**e**). Scale bar, 10 μm. **P* <0.01, compared with Con; ***P* <0.001, compared with TN (**f**). (**g**) Treatment of mice with high dose LPS activates renal PERK, but CHOP is suppressed and renal function is preserved in a TRIF-dependent manner. Wild-type or *Trif*$^{-/-}$ mice were injected intraperitoneally with 5 mg kg^{-1} LPS or vehicle control. Seven hours later, the kidneys were assayed for phospho-PERK and CHOP by immunoblot and for *CHOP* mRNA by RT–QPCR. **P* <0.01, compared with Con. Serum creatinine levels were measured at the indicated times after LPS treatment. **P* <0.01, compared with wild-type mice. For all graphs, data are presented as mean ± s.e.m., *n* = 3.

namely, induction by ER stress and suppression by LPS in wild-type but not *Trif*$^{-/-}$ mice (Fig. 3c).

Sepsis, as modelled by treatment with high dose LPS, leads to prolonged ER stress[12,13]. Successful host defence would probably call for prolonged UPR activation to handle increased protein load but suppression of prolonged CHOP expression. The pathway described here might enable high dose LPS to act as both an activator of the UPR and a selective suppressor of CHOP. To test this idea, wild-type and *Trif*$^{-/-}$ mice were injected with LPS (5 mg kg^{-1}), followed by examination of CHOP and phospho-eIF-2α expression and apoptosis in splenic macrophages. Treatment with this higher dose of LPS

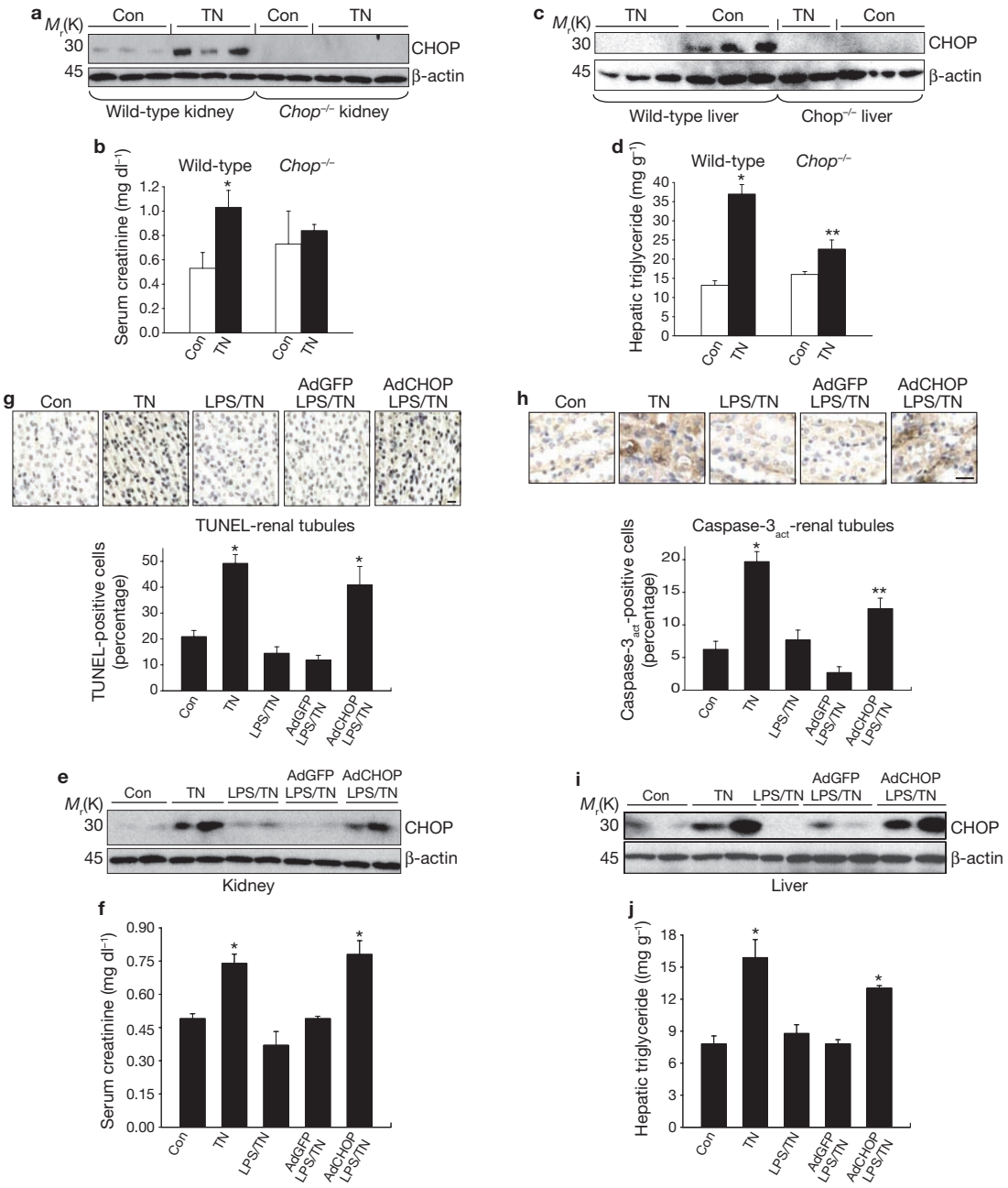

Figure 5 Protection from tunicamycin-induced renal dysfunction and hepatosteatosis by pretreatment with low dose LPS is due to suppression of CHOP. (**a**–**d**) Wild-type or *Chop*$^{-/-}$ mice were injected with tunicamycin (TN, 1 mg kg^{-1}) intraperitoneally and killed 48 h later. Kidneys were collected and subjected to immunoblot for CHOP and β-actin, and serum was assayed for creatinine concentration (**a**, **b**). *P <0.01, compared with Con; the two values for the *Chop*$^{-/-}$ mice were not significantly different. Livers were collected and subjected to immunoblot for CHOP and β-actin, and extracts were assayed for triglyceride mass (**c**, **d**). *P <0.001, compared with Con; **P <0.01, compared with wild-type TN value. (**e**–**j**) Mice were injected intravenously with LPS (80 μg kg^{-1}) or vehicle control intravenously for 2 consecutive days. On the second day, some mice were injected intravenously with either GFP-expressing adenovirus (AdGFP) or with CHOP-expressing adenovirus (AdCHOP). Mice were then injected with tunicamycin (TN 1 mg kg^{-1}) intraperitoneally and killed 48 h later. Expression of renal CHOP and serum creatinine levels were determined (**e**, **f**). *P <0.01, compared with Con and AdGFP. Renal tubule sections were stained for TUNEL or activated caspase-3 and quantified for percent-positive cells (**g**, **h**). *P <0.001, compared with Con; **P = 0.01, compared with control and <0.001, compared with AdGFP. Liver extracts were assayed for CHOP expression and triglyceride mass (**i**, **j**). *P <0.01, compared with Con and AdGFP. For all graphs, data are presented as mean ± s.e.m., n = 3. Scale bars, 20 μm (**g**, **h**).

resulted in only a slight increase in CHOP expression in wild-type mice at the 30-min time-point, and it was suppressed thereafter (Fig. 3d, left graph). By contrast, CHOP expression rose substantially after 30 min in the splenic macrophages of *Trif*$^{-/-}$ mice. Despite the lack of increase in CHOP expression in wild-type splenic macrophages, phospho-eIF-2α was markedly increased at both 30 min and 3 h (Fig. 3d, middle graph), consistent with the ability of high dose LPS to trigger the UPR and indicative of selective suppression of CHOP. The later rise in CHOP in *Trif*$^{-/-}$ but not wild-type splenic macrophages correlated with a sharp rise in apoptosis (Fig. 3d, right graph). Thus, during UPR activation by high dose LPS *in vivo*, splenic macrophage CHOP

is selectively suppressed in a TRIF-dependent manner, and this response is associated with protection against splenic macrophage apoptosis.

The renal proximal tubular epithelium responds to infectious insults through a TLR4-induced inflammatory response[26]. Moreover, the renal tubular epithelium is highly responsive to ER stress inducers, which is associated with renal dysfunction in a number of renal diseases[2,27]. We verified that both CHOP and phospho-eIF-2α were increased in the kidneys of tunicamycin-treated mice, with CHOP expression primarily in tubular cells (Fig. 4a, b). Pretreatment with low dose LPS markedly suppressed CHOP but not phospho-eIF-2α in the kidneys of wild-type mice, and CHOP suppression did not occur in *Trif*$^{-/-}$ mice (Fig. 4a). Two measures of renal function, serum creatinine and urine albumin:creatinine ratio, were abnormal in tunicamycin-treated wild-type mice but not in mice pretreated with LPS, and this protective effect of LPS was not seen in *Trif*$^{-/-}$ mice (Fig. 4c).

Hepatocytes also express TLR4 and respond to LPS[28,29], and are susceptible to ER stress-induced pathology, including CHOP-induced hepatic steatosis[30,31]. In tunicamycin-treated mice, CHOP was suppressed by low dose LPS pretreatment in wild-type but not *Trif*$^{-/-}$ liver (Fig. 4d). There was considerable basal expression of phospho-eIF-2α and it increased only slightly in the tunicamycin-treated mice, but it was not suppressed—and was actually slightly increased—by LPS (Fig. 4d). Livers from the tunicamycin-treated mice contained vacuolated hepatocytes that stained with Oil Red O, indicative of hepatosteatosis, which was suppressed by low dose LPS pretreatment (Fig. 4e). Consistent with these data, triglyceride and cholesterol content were higher in the livers of tunicamycin-treated mice, compared with control mice, and LPS pretreatment partially restored lipid levels to the control values in wild-type but not *Trif*$^{-/-}$ mice (Fig. 4f).

We re-examined the kidney findings in the model of ER stress induced by high dose LPS described above. Wild-type and *Trif*$^{-/-}$ mice were injected with LPS (5 mg kg^{-1}), followed by examination of renal CHOP expression and renal function. LPS treatment resulted in phosphorylation of PERK in both wild-type and *Trif*$^{-/-}$ kidneys (Fig. 4g). CHOP was not induced by LPS treatment in wild-type kidney, but was robust in the *Trif*$^{-/-}$ kidneys. Most importantly, serum creatinine did not rise in wild-type mice for as long as 7 h after treatment with high dose LPS, but serum creatinine did increase in the TRIF-deficient mice. To test the concept that the protective effect of LPS in tunicamycin-treated mice is caused by CHOP suppression, we compared tunicamycin-induced renal dysfunction and hepatosteatosis in wild-type, compared with *Chop*$^{-/-}$ mice. As above, tunicamycin treatment increased renal CHOP expression and serum creatinine, which was not seen in *Chop*$^{-/-}$ mice (Fig. 5a, b). Similarly, hepatic CHOP induction in tunicamycin-treated mice was associated with an increase in hepatic triglyceride content, which was abrogated in *Chop*$^{-/-}$ mice (Fig. 5c, d). We next used *CHOP* cDNA-containing adenovirus (adeno-CHOP) to restore CHOP expression in LPS-pretreated, ER-stressed mice to a level similar to that in mice not pretreated with LPS (Fig. 5e). Restoration of CHOP prevented LPS-mediated protection from renal dysfunction and tubular apoptosis (Fig. 5f–h). Treatment of non-ER-stressed mice with adeno-CHOP led to a 2–3-fold increase renal tubular apoptosis (data not shown). Adeno-CHOP also blocked LPS-mediated protection from hepatosteatosis in ER-stressed mice (Fig. 5i, j). Thus, suppression of CHOP expression is the mechanism by which low dose LPS prevents ER stress-induced renal tubular cell apoptosis, renal dysfunction and hepatosteatosis.

The coordinate expression of all three branches of the UPR contributes to adaptation to physiological stressors that would otherwise perturb the equilibrium of various ER functions[1]. The CHOP segment of the PERK branch presents a special situation in this process, because prolonged expression of CHOP triggers cell death[2–7]. Therefore, in cases of prolonged physiological ER stress, such as occurs during processes that entail a high level of protein synthesis, prolonged CHOP expression would not be desirable and, indeed, CHOP has been found to be suppressed under these conditions[10] (data herein). Several mechanisms have been proposed, including dephosphorylation of phospho-eIF-2α by CHOP-induced GADD34 (ref. 1), inhibition of the kinase domains of PKR and PERK by ATF6-induced P58^{IPK} (refs 32, 33), and suppression of all UPR branches by prior low levels of ER stress[6]. However, the lack of suppression of P-PERK and phospho-eIF-2α by LPS indicates that none of these mechanisms is responsible for ATF4–CHOP suppression by TLR–TRIF signalling. Indeed, the pathway described herein may uniquely allow cells to benefit from intact PERK activity[34] while avoiding the detrimental effects of CHOP.

The crucial role of TLRs in innate immunity has led us to speculate that the pathway revealed herein may protect cells from physiologically prolonged ER stress associated with host defence. Using high dose LPS as a model of sepsis, we showed that disabling the TLR–CHOP suppression pathway by TRIF deficiency resulted in detrimental effects in splenic macrophages and the kidney. However, other *in vivo* models will be needed to further expand the possible situations in which TLR–TRIF signalling is crucial to prevent the detrimental effects of prolonged ER stress. Moreover, once the downstream signalling pathways are further elucidated, other non-TLR pathways leading to suppression of ATF4 translation may be revealed, which in turn might suggest additional situations in which the fundamental principles of this pathway come into play *in vivo*.

A key mechanistic question that arises from our findings is how TLR–TRIF signalling suppresses ATF4 translation but not global translation in the face of phosphorylated eIF-2α. For phospho-eIF-2α to influence rates of translation initiation, the phosphorylation event must be sensed by eIF-2B, the GTP-exchange factor for eIF-2. Thus, it is possible that TLR–TRIF signalling may modulate such sensing by affecting known (that is, eIF-2B or eIF-2 components) or yet to be discovered components. Interference with this mechanism could account for the effects of LPS on both the normally observed upregulation of ATF4 and the global downregulation of protein synthesis.

In summary, the data presented in this report reveal a TLR–UPR cross-talk pathway in which pre-exposure of cells to activators of TLR–TRIF signalling selectively suppresses ATF4–CHOP expression in the setting of prolonged ER stress. This mechanism could uniquely enable the beneficial aspects of prolonged physiological ER stress without the detrimental effects of prolonged CHOP expression. Failure of this adaptive pathway may help explain diseases driven by excess CHOP expression[3,5,8], and selective targeting of this pathway may suggest new strategies to kill cancer cells that have adapted to prolonged ER stress[35].

METHODS

Methods and any associated references are available in the online version of the paper at http://www.nature.com/naturecellbiology/

Note: Supplementary Information is available on the Nature Cell Biology website.

ACKNOWLEDGMENTS

This work was supported by a German Research Foundation Grant (B.D.), NIH grants HL75662, HL57560 (I.T.), DK47119 and ES08681(D.R.). We thank Alice Prince and Vincent Racaniello (Columbia University) for helpful discussions related to the high-dose LPS mouse experiments and biological effects of TRIF signalling, respectively.

AUTHOR CONTRIBUTIONS

C.W., D.C., J.A. and B.D. performed the experiments and assisted with planning the experiments, data analysis and writing the manuscript; H.H. and K.A.F. assisted with planning the experiments and data analysis; D.R. assisted with planning the experiments, data analysis, and writing the manuscript; I.T. coordinated the project and assisted with planning the experiments, data analysis, and writing the manuscript. All authors discussed the results and manuscript text.

COMPETING FINANCIAL INTERESTS

The authors declare no competing financial interests.

Published online at http://www.nature.com/naturecellbiology/
Reprints and permissions information is available online at http://npg.nature.com/reprintsandpermissions/

1. Ron, D. & Walter, P. Signal integration in the endoplasmic reticulum unfolded protein response. *Nature Rev. Mol. Cell Biol.* **8,** 519–529 (2007).
2. Zinszner, H. *et al.* CHOP is implicated in programmed cell death in response to impaired function of the endoplasmic reticulum. *Genes Dev.* **12,** 982–995 (1998).
3. Oyadomari, S. *et al.* Targeted disruption of the *Chop* gene delays endoplasmic reticulum stress-mediated diabetes. *J. Clin. Invest.* **109,** 525–532 (2002).
4. Feng, B. *et al.* The endoplasmic reticulum is the site of cholesterol-induced cytotoxicity in macrophages. *Nature Cell Biol.* **5,** 781–792 (2003).
5. Song, B., Scheuner, D., Ron, D., Pennathur, S. & Kaufman, R. J. Chop deletion reduces oxidative stress, improves β cell function, and promotes cell survival in multiple mouse models of diabetes. *J. Clin. Invest.* **118,** 3378–3389 (2008).
6. Rutkowski, D. T. *et al.* Adaptation to ER stress is mediated by differential stabilities of pro-survival and pro-apoptotic mRNAs and proteins. *PLoS Biol.* 4, e374 (2006).
7. Lin, J. H. *et al.* IRE1 signaling affects cell fate during the unfolded protein response. *Science* **318,** 944–949 (2007).
8. Thorp, E. *et al.* Reduced apoptosis and plaque necrosis in advanced atherosclerotic lesions of *Apoe*$^{-/-}$ and *Ldlr*$^{-/-}$ mice lacking CHOP. *Cell Metabolism* **9,** 474–481 (2009).
9. Todd, D. J., Lee, A. H. & Glimcher, L. H. The endoplasmic reticulum stress response in immunity and autoimmunity. *Nature Rev. Immunol.* **8,** 663–674 (2008).
10. Skalet, A. H. *et al.* Rapid B cell receptor-induced unfolded protein response in nonsecretory B cells correlates with pro- versus anti-apoptotic cell fate. *J. Biol. Chem.* **280,** 39762–39771 (2005).
11. Kenny, E. F. & O'Neill, L. A. Signalling adaptors used by toll-like receptors: an update. *Cytokine* **43,** 342–349 (2008).
12. Ma, T. *et al.* The endoplasmic reticulum stress-mediated apoptosis signal pathway is involved in sepsis-induced abnormal lymphocyte apoptosis. *Eur. Surg. Res.* **41,** 219–225 (2008).
13. Hiramatsu, N., Kasai, A., Hayakawa, K., Yao, J. & Kitamura, M. Real-time detection and continuous monitoring of ER stress *in vitro* and *in vivo* by ES-TRAP: evidence for systemic, transient ER stress during endotoxemia. *Nucleic Acids Res.* 34, e93 (2006).
14. Li, Y. *et al.* Enrichment of endoplasmic reticulum with cholesterol inhibits SERCA2b activity in parallel with increased order of membrane lipids. Implications for depletion of ER calcium stores and apoptosis in cholesterol-loaded macrophages. *J. Biol. Chem.* **279,** 37030–37039 (2004).
15. Duksin, D., Seiberg, M. & Mahoney, W. C. Inhibition of protein glycosylation and selective cytotoxicity toward virally transformed fibroblasts caused by B3-tunicamycin. *Eur. J. Biochem.* **129,** 77–80 (1982).
16. Watowich, S. S. & Morimoto, R. I. Complex regulation of heat shock- and glucose-responsive genes in human cells. *Mol. Cell Biol.* **8,** 393–405 (1988).
17. Kedersha, N. L., Gupta, M., Li, W., Miller, I. & Anderson, P. RNA-binding proteins TIA-1 and TIAR link the phosphorylation of eIF-2α to the assembly of mammalian stress granules. *J Cell Biol.* **147,** 1431–1442 (1999).
18. Marciniak, S. J. *et al.* CHOP induces death by promoting protein synthesis and oxidation in the stressed endoplasmic reticulum. *Genes Dev.* **18,** 3066–3077 (2004).
19. Lee, Y. Y., Cevallos, R. C. & Jan, E. An upstream open reading frame regulates translation of GADD34 during cellular stresses that induce eIF2α phosphorylation. *J. Biol. Chem.* **284,** 6661–6673 (2009).
20. Lu, P. D. *et al.* Cytoprotection by pre-emptive conditional phosphorylation of translation initiation factor 2. *EMBO J.* **23,** 169–179 (2004).
21. Lu, P. D., Harding, H. P. & Ron, D. Translation reinitiation at alternative open reading frames regulates gene expression in an integrated stress response. *J. Cell Biol* **167,** 27–33 (2004).
22. Vattem, K. M. & Wek, R. C. Reinitiation involving upstream ORFs regulates ATF4 mRNA translation in mammalian cells. *Proc. Natl Acad. Sci. USA* **101,** 11269–11274 (2004).
23. Takaoka, A. *et al.* Integral role of IRF-5 in the gene induction programme activated by toll-like receptors. *Nature* **434,** 243–249 (2005).
24. Ouyang, X. *et al.* Cooperation between MyD88 and TRIF pathways in TLR synergy via IRF5 activation. *Biochem. Biophys. Res. Commun.* **354,** 1045–1051 (2007).
25. Fitzgerald, K. A. *et al.* LPS –TLR4 signaling to IRF-3/7 and NF-κB involves the toll adapters TRAM and TRIF. *J. Exp. Med.* **198,** 1043–1055 (2003).
26. Wolfs, T. G. *et al. In vivo* expression of toll-like receptor 2 and 4 by renal epithelial cells: IFN-γ and TNF-α mediated upregulation during inflammation. *J. Immunol.* **168,** 1286–1293 (2002).
27. Kitamura, M. Endoplasmic reticulum stress in the kidney. *Clin. Exp. Nephrol.* **12,** 317–325 (2008).
28. Nishimura, M. & Naito, S. Tissue-specific mRNA expression profiles of human toll-like receptors and related genes. *Biol. Pharm. Bull.* **28,** 886–892 (2005).
29. Seki, E. & Brenner, D. A. Toll-like receptors and adaptor molecules in liver disease: update. *Hepatology* **48,** 322–335 (2008).
30. Oyadomari, S., Harding, H. P., Zhang, Y., Oyadomari, M. & Ron, D. Dephosphorylation of translation initiation factor 2α enhances glucose tolerance and attenuates hepatosteatosis in mice. *Cell Metabolism* **7,** 520–532 (2008).
31. Rutkowski, D. T. *et al.* UPR pathways combine to prevent hepatic steatosis caused by ER stress-mediated suppression of transcriptional master regulators. *Dev. Cell* **15,** 829–840 (2008).
32. Yan, W. *et al.* Control of PERK eIF2α kinase activity by the endoplasmic reticulum stress-induced molecular chaperone P58IPK. *Proc. Natl Acad. Sci. USA* **99,** 15920–15925 (2002).
33. van, H. R., Martindale, J. L., Gorospe, M. & Holbrook, N. J. P58IPK, a novel endoplasmic reticulum stress-inducible protein and potential negative regulator of eIF2α signaling. *J. Biol. Chem.* **278,** 15558–15564 (2003).
34. Yamaguchi, Y. *et al.* Endoplasmic reticulum (ER) chaperone regulation and survival of cells compensating for deficiency in the ER stress response kinase, PERK. *J. Biol. Chem.* **283,** 17020–17029 (2008).
35. Boelens, J., Lust, S., Offner, F., Bracke, M. E. & Vanhoecke, B. W. Review. The endoplasmic reticulum: a target for new anticancer drugs. *In Vivo* **21,** 215–226 (2007).

METHODS

Materials. Tissue culture plastic was purchased from Fisher Scientific. Tissue culture medium and other tissue culture reagents were obtained from Invitrogen. All other chemicals and reagents, including tunicamycin and LPS were from Sigma-Aldrich, and all organic solvents were from Fisher Scientific. Antibodies against CHOP (sc-7351 antibody for immunoblotting and sc-575 for immunohistochemical and immunofluorescent staining; used at 1:500 and 1:250 dilutions, respectively) and ATF4 (1:500) were from Santa Cruz Biotechnology. Antibodies against phospho-PERK (1:500), IRE1α (1:500) and eIF-2α (1:500) were from Cell Signalling. Anti-phospho-eIF-2α (1:1,000) and anti-ATF6 (1:500) antibodies were purchased from Abcam and Imgenex, respectively. Horseradish peroxidase (HRP)-conjugated goat anti-rabbit IgG (1:3,000) and donkey anti-mouse IgG (1:3,000) were from Jackson ImmunoResearch. The primers for CHOP, ATF4 and cyclophilin A were synthesized by Invitrogen.

Mice. C57BL/6J mice were purchased from the Jackson Laboratory. *Chop*$^{-/-}$ mice were created as described previously[2] and bred 9 generations onto the C57BL6/J background. *Trif*$^{-/-}$ and *Tram*$^{-/-}$ were made as described previously[36,37] and crossed onto the C57BL6/J background. *Trif*$^{-/-}$*;Tram*$^{-/-}$ mice were generated by breeding *Trif*$^{-/-}$ and *Tram*$^{-/-}$ mice. *Irf3*$^{-/-}$, *Irf5*$^{-/-}$, *Irf7*$^{-/-}$ mice were created as described previoulsy[23,38,39].

Cells. Peritoneal macrophages from adult female C57BL/6J mice were harvested by peritoneal lavage four days after intraperitoneal injection of methyl-BSA in mice previously immunized with this antigen. The cells were maintained in culture as an adherent monolayer in medium containing DMEM, 10% FBS, and 20% L-cell-conditioned medium. The medium was replaced every 24 h until cells reached 90% confluence. Bone marrow macrophages from C57BL/6J and all other mutant mice were isolated by perfusing the medullary cavity of the femurs. Macrophages were maintained in medium containing DMEM, 10% FBS, and 20% L-cell-conditioned medium for 5 days. Cells were subcultured on day 6 for experiments. THP-1 monocytic cells (American Type Culture Collection) in RPMI-1640/10% FBS were plated at a density of 10^6 cells/35-mm dish and then incubated with medium containing 160 nM phorbol 12-myristate 13-acetate (PMA) to induce differentiation into macrophages. After 16 h, when the cells had become adherent, the PMA-containing medium was replaced with medium without PMA, and the experiment was conducted 24 h later. Murine embryonic fibroblasts (MEFs) were prepared from 13.5-day embryos as described previously[2] and cultured in DMEM/10% FBS. *Perk*$^{-/-}$ MEFs were stably transfected with FV2E-PERK as described previously[20] using a construct obtained from ARIAD Pharmaceuticals, who also supplied the semi-synthetic Fv2E dimerization reagent AP20187 (ref. 40).

Adenovirus and gene transfer. An adenoviral vector encoding the mouse CHOP gene (AdCHOP) and GFP (AdGFP) was constructed by ViraQuest. For *in vivo* gene delivery, mice were injected with 2×10^9 pfu/mouse of AdCHOP or AdGFP in 200 μL PBS via tail vein 24 h before injection with tunicamycin.

Immunoblot analysis. Immunoblots were conducted as described previously[4] with minor modifications. Briefly, cultured cells were lysed with Laemmli sample buffer (Bio-Rad), and mouse organs were homogenized in a lysis buffer containing 20 mM Tris (pH 7.4), 150 mM NaCl, 1% Triton-X, and phosphatase and protease inhibitor cocktails. For immunoblots of ATF4 and ATF6, nuclear fractions were prepared using a nuclear extraction kit (Panomics). Protein samples were separated by electrophoresis on Novex 4-20% Tris-glycine gels (Invitrogen) and transferred to nitrocellulose membranes. The membranes was probed with the indicated primary antibodies, and the protein bands were detected with HRP-conjugated secondary antibodies (Jackson ImmunoResearch) followed by ECL reagent (Pierce Lab). The membranes were reprobed with anti-β-actin or anti-nucleophosmin monoclonal antibodies for detecting differences in loading cellular or nuclear proteins, respectively. Densitometry analysis of the gels was carried out using ImageJ software from the NIH (http://rsbweb.nih.gov/ij/).

Detection of ATF4 and global protein translation. After the indicated cell incubations, the medium was switched to DMEM without methionine/cysteine. After 30 min, the cells were incubated with EasyTag ^{35}S-labelled methionine/cysteine mixture at 100 μCi ml^{-1} for 20 min. The cells were then lysed in a buffer containing 50 mM Tris-HCl (pH 7.5), 150 mM NaCl, 1mM EDTA, 1% NP-40, and a protease inhibitor cocktail. Proteins in the lysate were precipitated using trichloroacetic acid and radioactivity of the precipitated proteins was measured by a scintillation counter. An aliquot of cell lysate was subjected to immunoprecipitation using anti-ATF4 antibody. Radiolabelled proteins found in the immunoprecipitate were separated by electrophoresis on Novex 4–20% Tris-glycine gel (Invitrogen), and the dried gel was exposed to X-ray film for autoradiography.

RT–QPCR. Total RNA from peritoneal macrophages or tissues were isolated using Qiagen RNeasy mini kit. RNA was reverse-transcribed into cDNA using oligo-dT and M-MLV reverse transcriptase (Invitrogen). Real time quantitative PCR for CHOP and ATF4 was conducted using the SYBR green PCR reagent (Applied Biosystems) and Mx4000 Multiplex Quantitative PCR System (Stratagene). For CHOP (Ddit3), the forward and reverse primers were CCA CCA CAC CTG AAA GCA GAA and AGG TGA AAG GCA GGG ACT CA, respectively. For ATF4, the forward and reverse primers were GCA AGG AGG ATG CCT TTT C and GTT TCC AGG TCA TCC ATT CG, respectively. Cyclophilin A was used as an internal control, using the forward and reverse primers AAG AAG GCA TGA ACA TTG TGG AAG C and CGG AAA TGG TGA TCT TCT TGC TGG, respectively.

XBP-1 splicing. Total RNA from peritoneal macrophages was reverse-transcribed into cDNA. A segment of *XBP-1* mRNA was amplified using the forward primer AAC TCC AGC TAG AAA ATC AGC and the reverse primer ACC ACC ATG GAG AAG GCT GG. The spliced and unspliced XBP-1s were resolved by electrophoresis in a 1.5% agarose gel and visualized using ethidium bromide under UV light. GAPDH, using CCA TGG GAA GAT GTT CTG GG and CTC AGT GTA GCC CAG GAT GC as forward and reverse primers, respectively, was used as an internal standard to verify equal RT product loading for each experiment.

Histochemical analyses of mouse tissue. Kidney and liver were immersion-fixed in 10% neutral-buffered formalin overnight followed by embedding in paraffin. 7-μM cryosections (spleen) and 5-μm paraffin-embedded sections (kidney, liver) were immunostained using anti-CHOP antibody (Santa Cruz, SC-575) and rabbit ImmunoCruz staining system (Santa Cruz). Cryosections of the liver tissue were prepared and stained with Oil Red O to visualize lipid droplets. TUNEL staining of kidney and liver was performed on kidney sections by using GenScript TUNEL apoptosis detection kit. For spleen analysis, 7-μm cryosections were post-fixed in 10% neutral-buffered formalin and then permeabilized with ice-cold methanol for 5 min. Blocking was accomplished by incubation with 5% BSA in PBS for 2 h at room temperature. Immunofluorescent staining for CHOP or phospho-eIF-2α and CD68 was performed using anti-CHOP (Santa Cruz, SC-575) or anti-phospho-eIF-2α (Amgen) and anti-CD68 (Serotec) antibodies. AlexaFluor-595 goat anti-rabbit IgG (Invitrogen) and F(ab')$_2$-FITC goat anti-rat IgG (Santa Cruz) were used as secondary antibodies to visualize CHOP or phospho-eIF-2α and CD68, respectively. Sections were counterstained with DAPI and mounted with ProLong Gold anti-fade reagent (Invitrogen). Images were captured using Zeiss Axiovert 200M inverted microscope. For double staining of TUNEL and CD68, TUNEL staining was performed using In Situ Cell Death Detection Kit, TMR red (Roche Applied Science) before the immunofluorescence staining of CD68.

Lipid profile. Hepatic triglyceride and cholesterol levels were assessed by L-Type TG H and Cholesterol E kit (Wako Diagnostics), respectively. Lipid was extracted with chloroform: methanol: water ratio as 4:2:3 according to the method of Folch[41], and the dry lipid pellets were resuspended in 100% ethanol. Triglyceride and cholesterol levels were determined and normalized to liver wet weight.

Liver and kidney function tests. Serum was collected after centrifuging clotted blood at 3000*g* for 20 min. The creatinine concentration and ALT and AST activities in serum were measured by commercially available kits (Bio-quant). The albumin concentration in the urine was measured by a competitive ELISA (Exocell) and normalized to urine creatinine levels.

Statistics. Data are presented as mean ± s.e.m., with *n* noted in the individual figure legends. Analysis of variance followed by Holm-Sidak post-test (SigmaPlot 11.0) was used to determine statistical significance among all groups.

Accession codes. USCD-Nature Signaling Gateway (http@//www.signaling-gateway.org): **A002296** and **A002295**.

DOI: 10.1038/ncb1996

36. Yamamoto, M. *et al.* Role of adaptor TRIF in the MyD88-independent toll-like receptor signaling pathway. *Science* **301,** 640–643 (2003).
37. Yamamoto, M. *et al.* TRAM is specifically involved in the Toll-like receptor 4-mediated MyD88-independent signaling pathway. *Nature Immunol.* **4,** 1144–1150 (2003).
38. Sato, M. *et al.* Distinct and essential roles of transcription factors IRF-3 and IRF-7 in response to viruses for IFN-α/β gene induction. *Immunity* **13,** 539–548 (2000).
39. Honda, K. *et al.* IRF-7 is the master regulator of type-I interferon-dependent immune responses. *Nature* **434,** 772–777 (2005).
40. Feng, H., Zeng, Y., Whitesell, L. & Katsanis, E. Stressed apoptotic tumor cells express heat shock proteins and elicit tumor-specific immunity. *Blood* **97,** 3505–3512 (2001).
41. Folch, J., Less, M. & Sloane-Stanley, G. H. A simple method for the isolation and purification of total lipids from animal tissues. *J. Biol. Chem.* **226,** 497–509 (1957).

nature cell biology

DOI: 10.1038/ncb1996

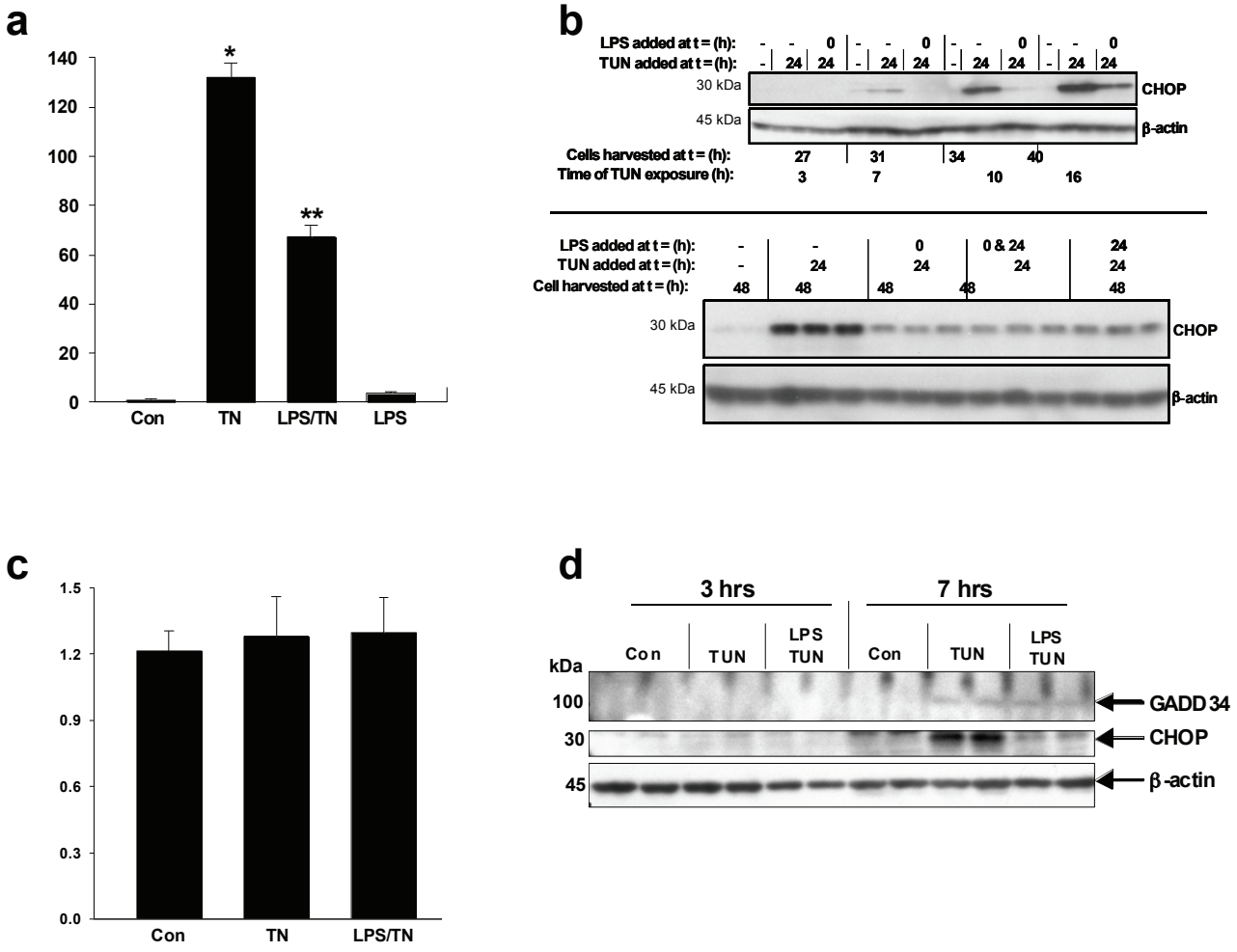

Figure S1 LPS suppresses tunicamycin-induced CHOP mRNA and protein, but not ATF4 mRNA or GADD34. **a** CHOP mRNA was quantified by RT-QPCR in untreated macrophages (Con); macrophages treated for 7 h with 1 μg/ml tunicamycin; macrophages pre-treated for 24 h with 1 ng/ml LPS prior to tunicamycin treatment; or in macrophages treated for 24 h with LPS alone. *, $P < 0.02$ vs. Con; **, $P < 0.008$ vs. TN. **b** In the upper blot, macrophages were exposed to one dose of 1 ng/ml LPS at time = 0 h and then treated with 1 μg/ml tunicamycin at time = 24 h. At 3, 7, 10, and 16 h after the tunicamycin treatment, cell extracts were immunoblotted for CHOP and β-actin. In the lower blot, macrophages were exposed to one dose of 1 ng/ml LPS at time = 0 h, 24 h, or both 0 and 24 h. The cells then treated with 1 μg/ml tunicamycin at time = 24 h, and at time= 48 h, cell extracts were immunoblotted for CHOP and β-actin. **c** Total RNA was extracted and subjected to quantitative RT-PCR using primers for ATF4 and a control mRNA, cyclophilin A. The data are expressed as the level of ATF4 mRNA relative to that of cyclophilin A. None of the values were statistically different from each other. **d** GADD34 and CHOP expression were determined in untreated macrophages (Con); macrophages treated for 3 or 7 h with 1 μg/ml tunicamycin; or macrophages pre-treated for 24 h with 1 ng/ml LPS prior to tunicamycin treatment. For the graphs in a and c, data are presented as mean ± S.E.M., n = 3.

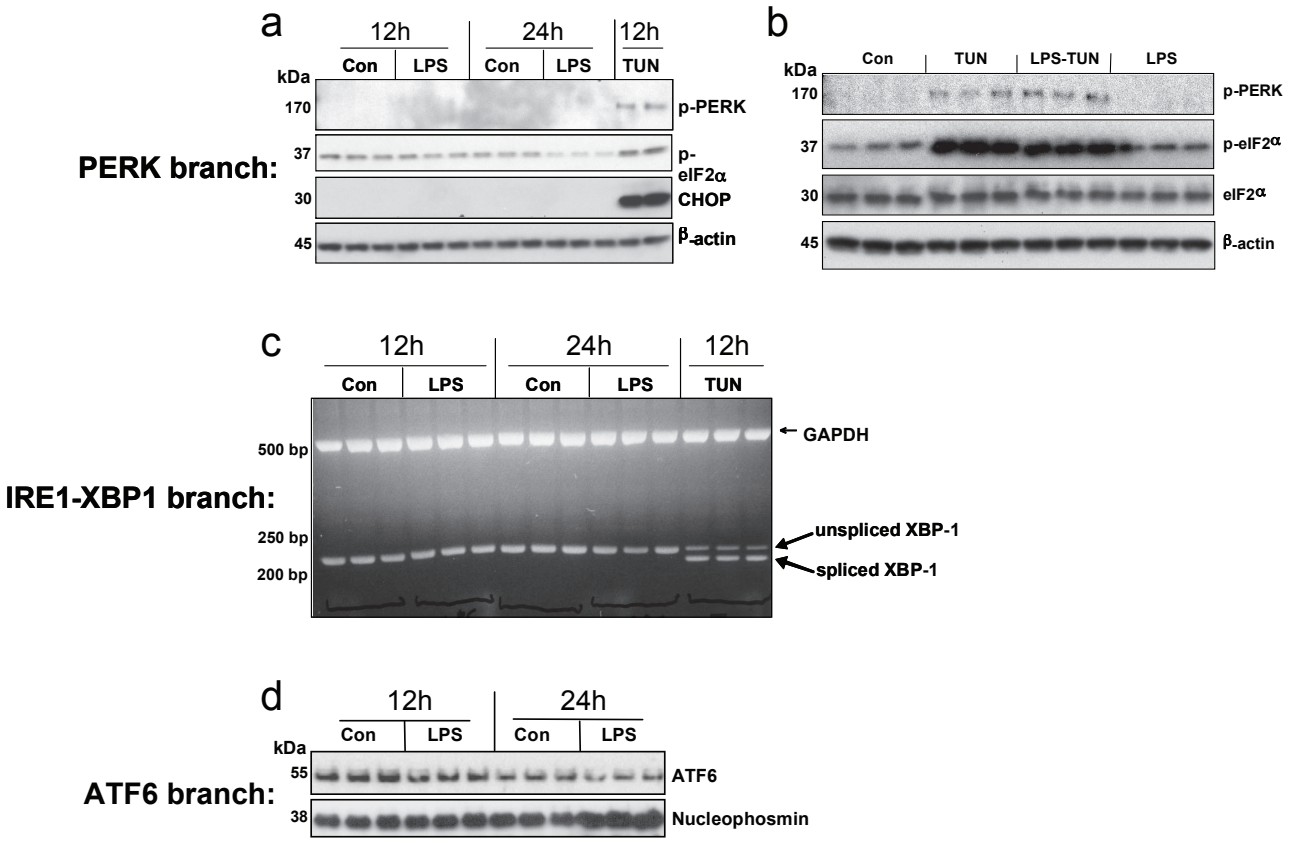

Figure S2 None of the three branches of the UPR are activated by 1 ng/ml LPS. **a, c, d** Macrophages were incubated for 12 or 24 h in medium alone or in medium containing 1 ng/ml LPS. In those cases where no basal signal was seen, a 12-h incubation with 1 μg/ml tunicamycin (TUN) was used as a positive control. Whole-cell extracts were assayed by immunoblot for P-PERK, P-eIF2a, CHOP, and β-actin (loading control); RNA was assayed by RT-PCR for unspliced and spliced XBP-1; and nuclear extracts were assayed by immunoblot for cleaved ATF6 and nucleophosmin (nuclear loading control). As noted in the text and seen in Fig. 1H, macrophages demonstrate basal cleaved ATF6, which is shown here to diminish after 24 h in culture. However, at neither timepoint was ATF6 increased above control by LPS. **b** Macrophages were pre-incubated for 24 h in the absence or presence of 1 ng/ml LPS and then treated for 7 h with 1 μg/ml tunicamycin where indicated. Cell extracts were immunoblotted using antibodies against phospho-PERK, phospho-eIF-2α, total eIF-2α, and β-actin.

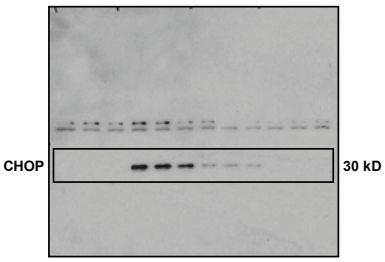

anti-CHOP WB for TN: Figure 1a

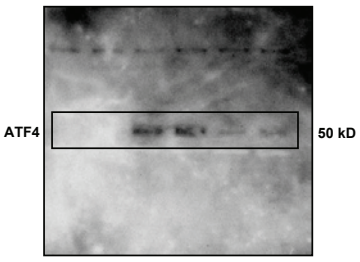

anti-ATF4 WB for TN: Figure 1b

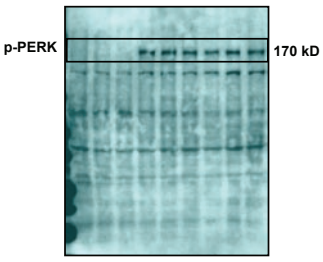

anti-p-PERK WB: Figure 1c

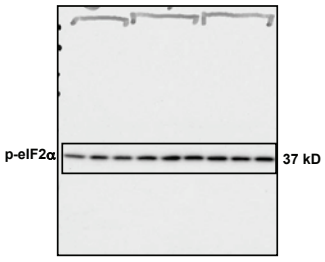

anti-p-eIF2α WB: Figure 1c

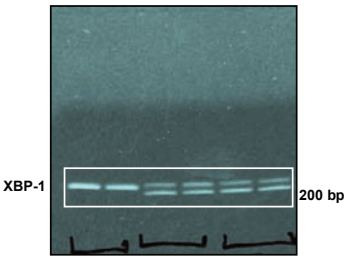

XBP-1 PCR: Figure 1e

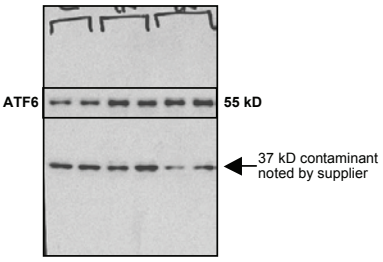

anti-ATF6 WB: Figure 1f

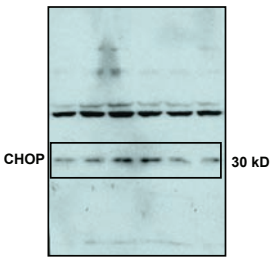

anti-CHOP WB for FV2E-PERK MEFs: Figure 1g

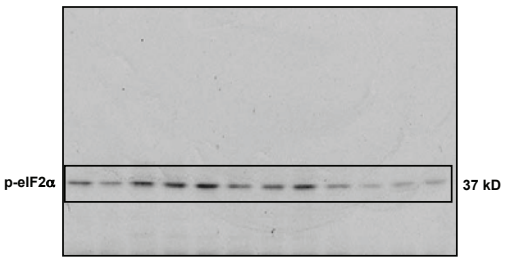

anti-p-eIF2α WB: Figure 1h

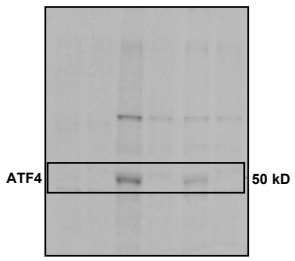

ATF4 autoradiogram: Figure 1i

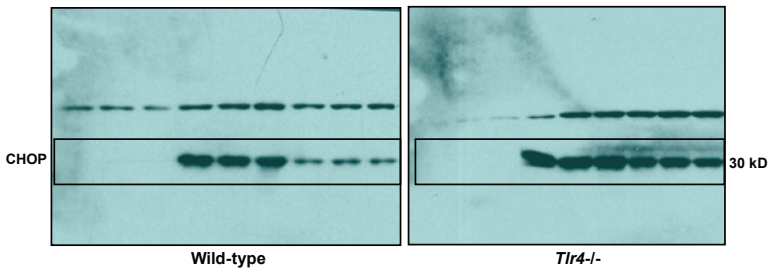

anti-CHOP WB: Figure 2a

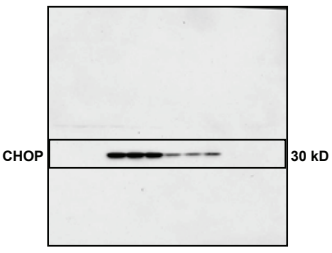

anti-CHOP WB (7h): Figure 2d

Figure S3 Full scans of Western blots from key figures